RSC Advances

PAPER

View Article Online
View Journal | View Issue

Cite this: *RSC Adv.*, 2021, **11**, 28313

Riboflavin based conjugated biomolecule for ultrasensitive detection of nitrophenols†

Bandita Kalita, Priyanka Dutta and Neelotpal Sen Sarma *

Received 7th June 2021
Accepted 17th August 2021

DOI: 10.1039/d1ra04403f

rsc.li/rsc-advances

Real time detection of explosive compounds in today's time is of utmost necessity due to security and severe environmental safety issues. Herein, we have synthesized a biobased conjugated molecular system from riboflavin and L-cystine utilized it for detecting picric acid in trace amount using optical sensing technique. The bioconjugate probe showed high quenching efficiency towards picric acid, which is 92.2%. In depth mechanistic study showed that ground state electrostatic interaction and inner filter effect are the factors leading to the diminishing of the probe's fluorescence intensity on addition of trace amount of the nitrophenol, picric acid. The detection limit of the conjugate is 0.37 nM which is extremely low and highly desirable for clinical applications of this system.

Introduction

Rapid and selective detection of explosive compounds has gathered much interest due to its usefulness in homeland security, remediation of explosive sites, forensic and criminal investigations.[1–3] Common techniques of detection involve sniffer dogs and metal detectors. But trace amount of organic explosive compounds are difficult to detect *via* such techniques.[4] Picric Acid (PA), whose IUPAC name is 2,4,6-trinitrophenol, a polynitrated chemical highly explosive in nature. The explosive nature of PA is apparently found to be higher than that of the common powerful explosive, TNT. PA is also extensively used in manufacturing units of dyes, fireworks as well as rocket fuels.[5,6] The nitroaromatic chemicals (NACs) possess electron-withdrawing capacity and thus produce harmful gas vapors. PA dissolves in water and hence possesses a substantial threat by getting released into the environment. It is potentially hazardous for infected waterbody dependent wildlife and human beings. Also, it is very toxic in case of contact with eyes and skin, ingestion, or inhalation and can result in lung damage, difficulty in breathing, loss of consciousness, or even death.[7] According to the precautionary measures releases for handling of picric acid, overexposure to this acid can cause anemia, liver function disorder, and cataracts.[8,9] Therefore, development of newer materials and advanced methods for the detection of this compound from the environment has garnered a lot of attention in recent times. The detection of picric acid mostly happens in outdoor places like blast sites, minefield, *etc.*[10,11] Here, along with PA, various other pollutants remain present, thereby making the detection of PA a very difficult as well as a necessary task. For this purpose, the fluorescence technique is widely used. It has advantage over other techniques because of its rapid response, easy sample preparation and sensitivity.[12] Different techniques were used for the detection of PA, like colorimetry,[13] but fluorescence[14–17] has been predominantly used for its quick response, easy sample preparation, *etc.* Other methods involve gas chromatography,[18] voltammetry,[19] cyclic voltammetry technique,[20] surface-enhanced Raman spectroscopy,[21,22] fiber-optics detection method,[23] energy-dispersive XRD,[24] nuclear quadrupole resonance,[25] amperometry,[26] and gas chromatography mass spectrometer (GCMS),[27] electroluminescence,[28] electrochemical.[29] Keeping in mind all of these circumstances, we have synthesized a biobased conjugate riboflavin–cystine (RC) *via* Fischer esterification reaction for a fluorescent quenching detection of picric acid. This RC acts as a novel, less expensive, selective and highly sensitive sensor with riboflavin being used as the fluorescent tag molecule. Riboflavin is a yellowish-green fluorescent compound isolated from an enzyme,[30] found in green, leafy vegetables bounded to proteins. It is also present in different amounts in natural unprocessed foods as well as dairy products, meat and fruits.[31,32] Riboflavin transfers single electron, hydrogen atom and hydride ions to the substrate, contributing in a redox reaction in biological systems. Riboflavin shows strong absorption peaks at 223 nm, 267 nm, 372 nm and 444 nm in the UV-vis regions when dissolved in water and simultaneously gets degraded to different' photoproducts on exposure to light.[33] Riboflavin forms molecular complexes with complex molecules[34] and this slows down its rate of degradation reactions.[35,36] Riboflavin upon absorption of light undergoes a change in its molecular state and gets excited. These states then emits fluorescence to come back to their original ground state.[37,38] Our developed fluorescent conjugate RC showed

Advanced Materials Laboratory, Physical Sciences Division, Institute of Advanced Study in Science and Technology, Guwahati, 781035, Assam, India. E-mail: neelot@iasst.gov.in

† Electronic supplementary information (ESI) available. See DOI: 10.1039/d1ra04403f

significant photoluminescence quenching towards PA. The quenching phenomenon is proposed to be a ground state electrostatic interaction of the synthesized conjugate and PA. Furthermore, the remarkably low detection limit makes it an extremely suitable system for effective sensing of picric acid.

Experimental

Materials and methods

Riboflavin (Merck), BOC-L-cystine (Sigma), ethyl methyl ketone (Merck), ethanol (Merck), *p*-toluene sulfonic acid (Merck) were used. The analyte picric acid (PA) was provided by Sigma. 3,5-Dinitrosalicylic acid (DNSA), dinitro benzene (DNB), 2-nitrophenol (2NP), nitrobenzene (NB), 4-nitrophenol (4NP), nitromethane (NM), nitroethane (NE), benzoic acid (BA) and chloroform were obtained from Merck.

CAUTION! The nitroaromatic compounds need to be handled very carefully. Picric acid must be kept in purified water. For humans, the safety limit of exposure to PA is 0.1 mg m^{-3}.

FTIR, TGA and XRD. The samples were analysed using Fourier transform infrared (FTIR) spectra within the range 600–4000 cm^{-1} and were with 64 scans in a KBr matrix. PerkinElmer Spectrum Two FT-IR Spectrophotometer was used for this purpose. The thermogravimetric analysis of the conjugate was checked in the PerkinElmer TGA 4000. It was set at a constant N_2 flow with a flow rate of 20 mL min^{-1} with a heating rate of 10 °C min^{-1} in a temperature range of 35–800 °C. The X-ray diffraction (XRD) study was done using a Bruker D8 Advance diffractometer with Cu Kα (λ = 1.54 Å) as the incident ray operating at 40 kV and 40 mA in the angular range 2θ = 5–80°.

Sample preparation for dynamic light scattering (DLS) and spectroscopic studies. The conjugate sample was dissolved in ethanol and was diluted in purified water. This was then used for the DLS study and other spectroscopic studies. PA was dissolved in distilled water and was used for the PL experiments. For real-time analysis, picric acid solutions were prepared in running water from the water dispersal system at IASST and UV–RO filtered drinking water. Zeta potential was checked at 25 °C in Malvern Nano ZS90.

Spectroscopic experiments and TRPL. The UV studies were done in the 1800 SHIMADZU UV-vis spectrophotometer at 25 °C. The PL spectra were recorded using a halogen lamp fitted Cary Eclipse spectrophotometer. The slit widths for excitation and emission were kept at 5 nm. Quartz cells were taken for spectral measurements. A fluorescent turn-on, which refers to the increase in the intensity of the PL spectra, or a fluorescent turn-off, which refers to the decrease in the intensity of the PL spectra of the probe on addition of the analytes is checked. Time-resolved photoluminescence (TRPL) study is done using the Edinburg Instruments FSP920, Picosecond Time-resolved cum Steady State Luminescence Spectrometer with an excitation LED source of wavelength 290 nm.

Synthesis of conjugate riboflavin–cystine (RC)

Riboflavin (0.01 mol, 3.76 g) and BOC-L-cystine (0.01 mol, 2.21 g) were dissolved in 250 mL of ethyl methyl ketone (EMK) along with 0.05 g of *para*-toluene sulfonic acid (*p*-TSOH). This mixture was allowed to cool to room temperature, and was then extracted by precipitating it in a large volume of ice-cooled water. This reaction is called the Fischer esterification[39] and it led to the formation of the ester which was further mixed with *p*-TSOH in a beaker and was irradiated under microwave for half a minute.[40] This mixture was let to cool down, filtered and washed with water and stored after vacuum drying. This product was termed as riboflavin–cystine (RC) and the synthesis is shown as Scheme 1.

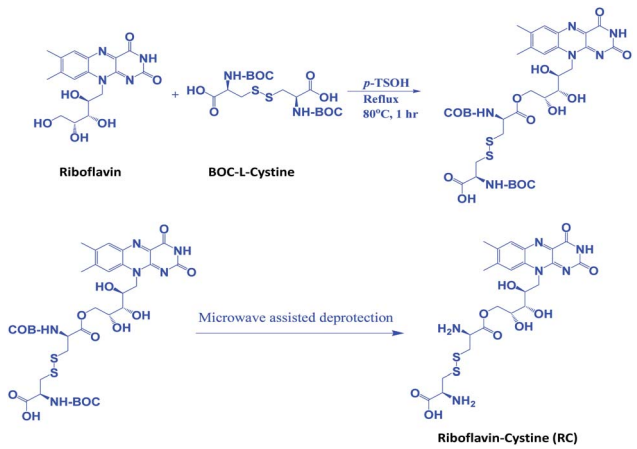

Scheme 1 Reaction scheme of the synthesis of bio conjugate RC.

A 0.1 M picric acid solution was prepared by having 2.3 g of PA in 100 mL of distilled water and then diluted for desired concentrations.

Results and discussion

Synthesis of the bio-conjugate RC

Fourier transform infrared spectroscopy (FTIR). The chemical composition of the conjugate RC is evaluated by doing the infrared spectroscopy study. In Fig. 1A, the peak at 1734 cm^{-1} confirms the formation of the ester group. This is because of the symmetric stretching of the C=O ester group. The peak at 1188 cm^{-1} is from the stretching vibration of the functional group C–O of the ester along with the peaks at 1645 cm^{-1} and 1244 cm^{-1} which denotes the primary amine group's bending vibration and that of the C–N of the amino acid moiety.

Thermal analysis and crystalline properties. Fig. 1B depicts the TGA curves of the conjugate RC and the parent compound riboflavin. It was found that the conjugate is stable for more than 240 °C, which is a desirable property for usage in high temperature environment. Moreover, the comparatively lower thermal stability of the conjugate as that of the parent compound confirms the formation of ester linkage.[41] Complete degradation of the compounds occur at around 700 °C. Also, from the X-ray diffraction (XRD) plot, it was seen that the conjugate is crystalline in nature as evident from the sharp peak at 2θ = 18° in Fig. S1 in ESI.†

Photophysical properties. RC exhibited a strong absorption peak with absorption maxima (λ_{max}) at 445 nm as well as

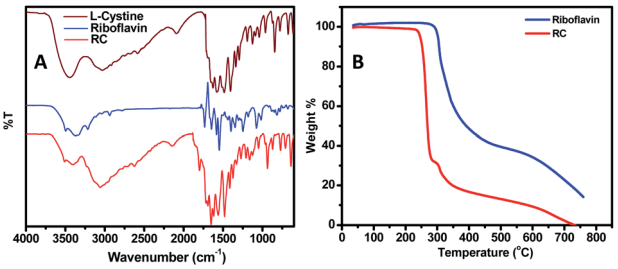

Fig. 1 (A) Comparative FTIR of L-cystine, riboflavin and RC (B) TGA of riboflavin and RC.

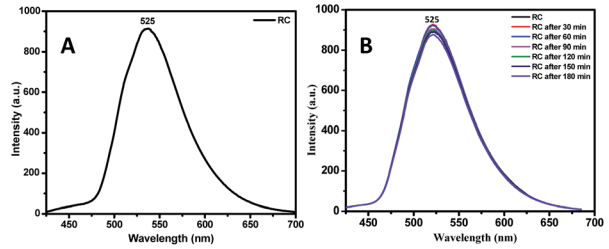

Fig. 2 (A) Emission of RC and (B) photostability of RC.

a strong emission peak at λ_{max} 525 nm on excitation at 420 nm. The absorption of the conjugate is shown in Fig. S2 in the ESI.† The emission spectra of the conjugate RC is depicted in Fig. 2A. The photostability study of 7th conjugate RC in ethanol–water mixture at room temperature, 25 °C is depicted in Fig. 2B.

Sensitivity studies. The conjugate RC was tested for its sensitivity in the presence of picric acid and other nitroaromatic chemicals. Fluorescence titration for solution of RC (0.01 mM) with solution of PA revealed that it is comparatively much more sensitive towards PA than to other chemicals. The PL intensity of the conjugate gradually decreases upon the addition of picric acid. The quenching efficiency is found to be 92.2%. The interference study was done with the compounds 2-nitrophenol (2NP), 4-nitrophenol (4NP), 3,5-dinitrosalicylic acid (DNSA), 1,4-dinitrobenzene (DNB), nitrobenzene (NB), benzoic acid (BA), chloroform, nitromethane (NM), and nitroethane (NE). It was found that the PL intensity of the conjugate does differ in the presence of these analytes but it was prominent that the sensitivity of RC towards picric acid is much more compared to the above-mentioned analytes. Fig. 3(A–F) shows the PL quenching of RC with various nitroaromatic compounds.

For a good chemosensor, the sensor has to be selective towards a specific type of analyte. The selectivity of the conjugate RC was tested along with various metal ions like Li^+, Na^+, Ba^{2+}, Ag^{2+}, Ca^{2+}, Co^{2+}, Cu^{2+}, Pb^{2+}, Zn^{2+}, and Zn^{2+} ions. The fluorescence intensity of the bioconjugate RC hardly changes in the presence of metal ions. Fig. 4(A and B) depicts the conjugates selectivity towards PA and other interferents. It was found that these chemicals effect very less in the PL quenching efficiency of the conjugate. This study showed the impact of all these chemicals, or interferents in the quenching phenomenon of PA, as shown in Fig. 4(C and D). As seen in Fig. 4(C and D), the

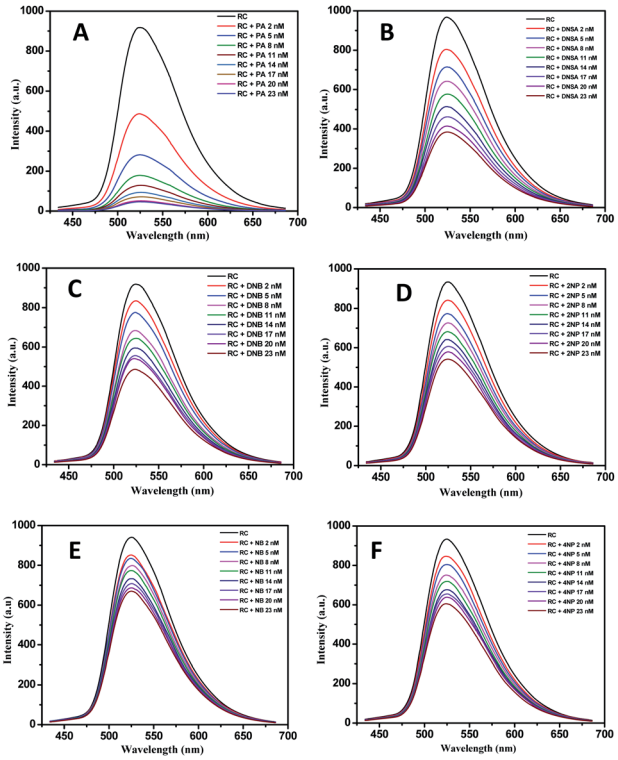

Fig. 3 PL quenching of RC with different nitroaromatics (A) picric acid (B) dinitrosalicylic acid (C) dinitrobenzene (D) 2-nitrophenol (E) nitrobenzene and (F) 4-nitrophenol.

picric acid is quenched to the highest degree. Hence, even in the presence of the other nitroaromatics, as well as the metal ions, the efficiency of PA outweighs that of the interferents. Also, the lack of proper binding sites in the metal ions adds to the less interference of the metal ions in the PL quenching of RC. This is a desirable property, allowing us to detect PA even in the presence of other nitroaromatics, or interfering metal ions.[42]

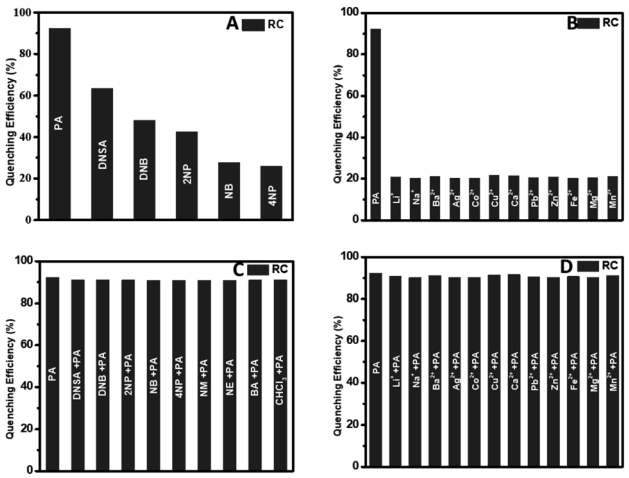

Fig. 4 Selectivity study of RC in the presence of (A) nitroaromatic compounds (B) metal ions, interference of (C) chemicals (D) 10 μM solution of metal ions in PA sensing.

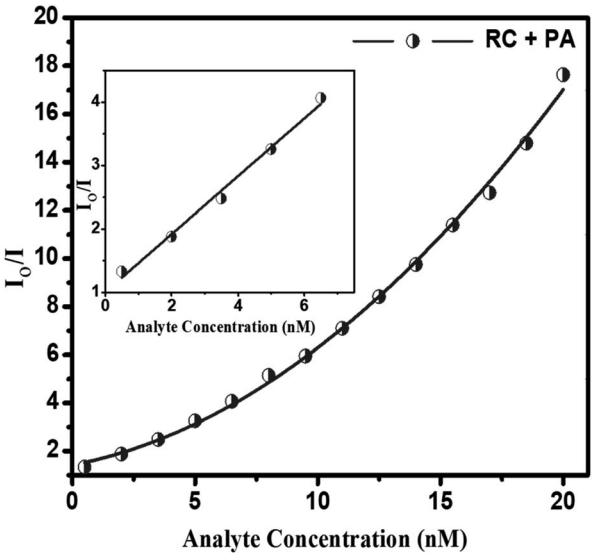

Fig. 5 Stern–Volmer plot for RC with PA.

Stern–Volmer plots and TRPL study. The Stern–Volmer (SV) equation was used to understand the quenching mechanism of the conjugate's fluorescence intensity by the analyte, where I_o is the fluorescence intensity of the plain conjugate and I is the fluorescence intensities of the conjugate after addition of NACs to it. [Q] is the analyte's's concentration along with K_{SV} being the Stern–Volmer constant.

$$I_o/I = 1 + K_{sv}[Q]$$

The SV plot predicts the quenching mechanism in the sensor system. The K_{SV} can be determined from the slope of the plot.[43]

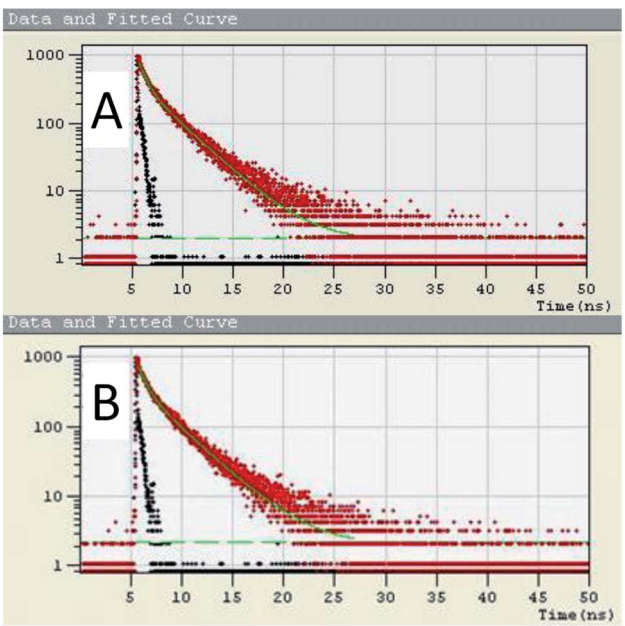

Fig. 6 TRPL spectra of RC (A) before and (B) after the addition of PA.

The value of the K_{SV} depicts the efficiency of the quencher to the fluorophores.[44] The $(I_o/I) - 1$ *versus* concentration of the quencher [Q] in Fig. 5 gives the SV plot which is a non-linear curve, which is comparatively linear at regions of lower concentration of analyte. This curve then bends upwards at higher concentration. The curving away from linearity indicates that either one or coexistence of both the quenching mechanisms, *i.e.* static as well as dynamic exists. The Stern–Volmer constant from the linear fitted Stern–Volmer plot is calculated from the slope. The SV binding constants (K_{SV}) of the conjugate is found to be 2.188×10^9. To dig deeper into the mechanism of the quenching phenomenon, the time-resolved photoluminescence (TRPL) study was carried out. From the TRPL studies, details of the interaction of the donor (RC) and donor–acceptor complex (RC + PA) were found. Fig. 6(A and B) shows the TRPL spectra of the conjugate RC before and after interaction with PA. For RC, in Fig. 6A, the τ value is 0.621 ns and χ^2 is 1.027, whereas, for RC + PA, in Fig. 6B, the τ value is 0.697 ns and χ^2 is 1.059. The fluorescence lifetime of the conjugate remained unchanged even after the addition of picric acid, which suggests that ground state electrostatic interactions took place for static quenching phenomenon.

From the SV plot and TRPL measurements, the mechanism of the sensing is proposed to be a ground state electrostatic interaction between the conjugate and the analyte, PA. The conjugate RC's high sensitivity towards PA and the Stern–Volmer plot's nonlinearity suggests the occurrence of either Forster resonance energy transfer, FRET or Inner Filter Effect (IFE). The probability of an excited-state energy transfer *via* FRET is not considered as we find that the lifetime of the probes remained unchanged upon addition of picric acid. The reason for this quenching mechanism hence is a strong inner filter effect, along with some electrostatic interactions. IFE refers to reabsorption of the emitted light of the conjugate by the quencher. Fig. 7 shows an overlap between the normalized emission band of the conjugate and the normalized absorption band of picric acid. Due to this overlap, the sensor and the

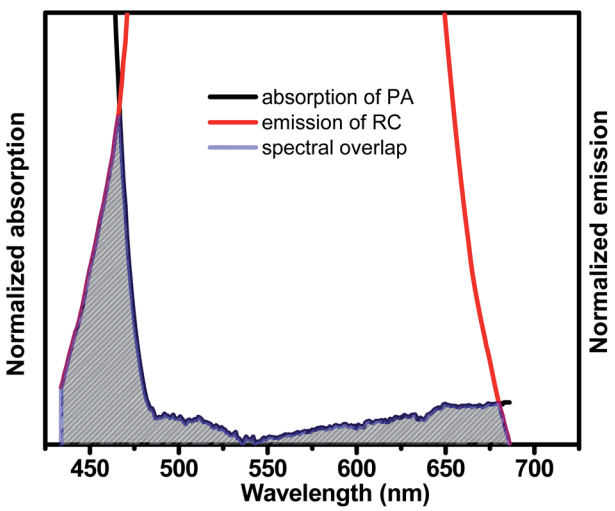

Fig. 7 Spectral overlap of absorption of PA and emission of RC.

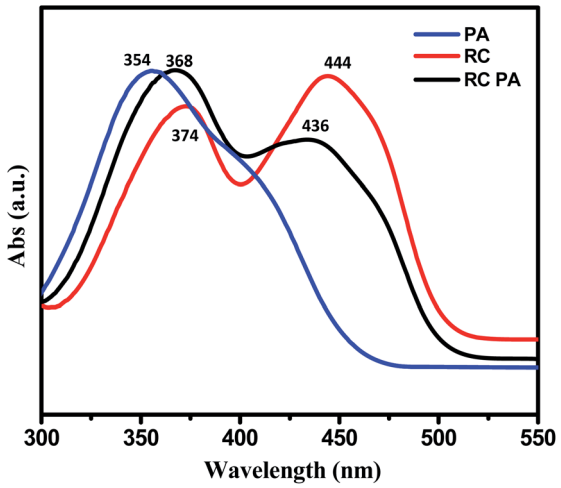

Fig. 8 UV spectroscopy of 0.1 mM RC, 0.01 mM picric acid and 0.1 mM RC after addition of 20 nM picric acid.

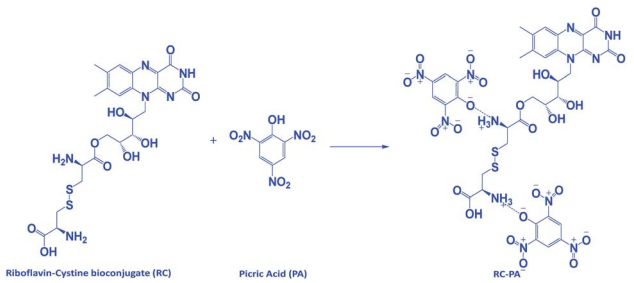

Scheme 2 Mechanistic insight towards the interaction between RC and PA.

analyte's reacting units get comparatively closer to each other, which leads to the increase in the interaction between the conjugate and the analyte.

We believe that electrostatic interactions like the H-bonding between $-NH_2$ of the conjugate and the analyte's –OH group happens, which leads to ground state electrostatic interactions.[45] The presence of the $-NO_2$ groups makes the –OH group of the analyte PA highly acidic and hence reacts easily with the basic amine group of RC. To further see the possibility of interaction of the conjugate with acid, we carried out PL tests with benzoic acid wherein we recorded no fluorescence intensity change. Also, aliphatic nitro compounds were used to check the selectivity of the conjugate towards nitroaromatic compounds as given in Fig. S3 in the ESI.† The UV spectroscopic measurements as given in Fig. 8 gave more insights towards this. A significant decrease in the absorbance peak was evident from the UV-vis studies. The peak of RC at 445 nm came down after the addition of PA. This was followed by the formation of the absorption peak for PA at 350 nm as shown in Fig. S4 in ESI.† The λ_{max} value of the conjugate remained unchanged upon the addition of PA which also proves the point that no ground-state complex formation took place. The presence of electrostatic interactions such as H-bonding between the –OH group of picric acid and the –NH group of the basic conjugate

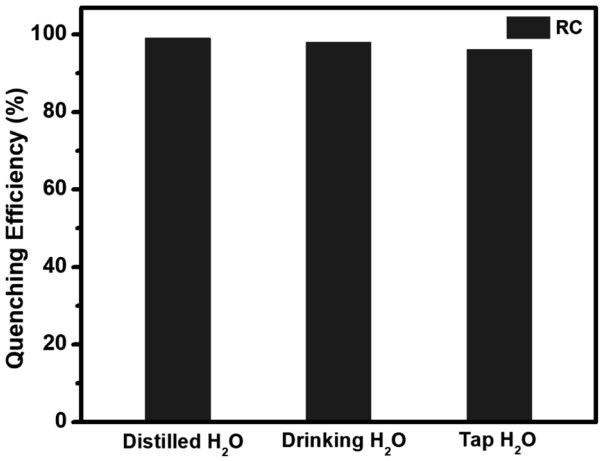

Fig. 9 Real-time analysis of PA in water.

are the reason for fluorescence quenching.[46,47] The electrostatic interaction of the conjugate with picric acid is represented in Scheme 2.

The zeta potential (ζ) value shows the electrostatic interaction, given in Fig. S5 in the ESI.† The ζ value of picric acid is −13.7 mV. The ζ value of the conjugate RC is −13.4 mV. This then reduces to −3.34 mV on adding picric acid. This shows that an electrostatic interaction takes place between the conjugate and the analyte.

Sensing experiments in real samples. The quenching efficiency of RC for picric acid was checked by preparing the PA solutions prepared in running tap water and UV/RO filtered drinking water. The efficiency of the probe was found to be almost similar in all of the cases. This is due to the lack of proper binding sites in the conjugate towards metal ions which senses the picric acid selectively. This increases the potential of the conjugate for its application as an efficient sensing material for picric acid. The comparative data in real samples is given in Fig. 9.

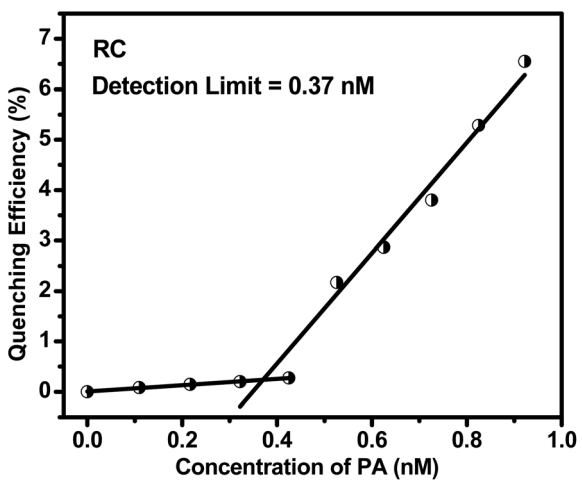

Fig. 10 Limit of detection of RC for PA.

Table 1 Comparative study of limit of detection (LOD) of our developed sensor system over already reported PA sensors

Sl no.	Sensor system	LOD for PA	Method	Ref.
1	Anthracene-bridged AA-type bi-arm poly(*N*-vinylpyrrolidone)	0.006 mM	Fluorescence turn off	48
2	Bluish green fluorescent histidine	2.7 μM	Fluorescence turn off	49
3	*N*,*N*′-di-[2-hydroxy-3-methoxy-benzylidene]-benzene-1,4-diamine (DBA)	72 nM	Fluorescence turn off	50
4	Rhodamine dye-containing isonicotinic hydrazide	37.3 nM	Fluorescence turn on	51
5	*Para*-nitrophenyl triazole trindane platform based C_{3v}-symmetric tripodal supramolecular receptor	421 nM	Fluorescence turn off	52
6	PPA-CSQ	0.65 nM	Fluorescence turn off	42
7	CQDs/PANI nanocomposite	0.056 μM	Fluorescence turn off	53
8	RC	0.37 nM	Fluorescence turn off	(Our system)

Limit of detection (LOD). The quenching efficiency of the conjugate is given by the conjugate's capability of having an extremely low limit of detection towards picric acid, given in Fig. 10. The limit of detection was in the nanomolar range being 0.37 nM picric acid. This detection limit is quite low compared to a few reported sensory systems given in Table 1.

Conclusions

In the summary we can conclude that in this work a bio-based riboflavin–cystine (RC) is synthesized in a very simple synthesis and purification method. The result as obtained from fluorescence spectroscopy indicates that the compound is highly efficient and sensitive towards selective detection of nitroaromatic chemicals in general and picric acid in particular in aqueous medium. The synthesis process involves riboflavin and L-BOC cystine as the ingredients. The florescent nature of RC diminishes upon the addition of PA with an immense low concentration of 2 nM. We have compared the quenching efficiency of our material with that of few reported one and found that it is remarkably high. The calculated LOD is 0.37 nM only. The sensing of PA is equally efficient in real samples and so will help in the detection of PA in practical field.

Author contributions

Bandita Kalita conceived the idea, did all the experiments and wrote the manuscript. Priyanka Dutta assisted during the initial work plan and helped in the determination of the detection limit. Neelotpal Sen Sarma supervised the whole work.

Conflicts of interest

There are no conflicts to declare.

Acknowledgements

The authors thank the Department of Science and Technology, Government of India, and IASST, Guwahati, for financial support; CIF IASST and CIF IITG for characterization and analysis. The authors also acknowledge Gautomi Gogoi for her immense help in designing the three dimensional (3D) molecular structures, Samiran Upadhyaya, Kangkan Jyoti Goswami and Hridoy Jyoti Bora for their input in formatting the manuscript, Dr Anamika Kalita and Dr Bedanta Gogoi for their valuable suggestions regarding the scheme of this work.

References

1 H. Sohn, M. J. Sailor, D. Magde and W. C. Trogler, *J. Am. Chem. Soc.*, 2003, **125**, 3821–3830.
2 S. J. Toal and W. C. Trogler, *J. Mater. Chem.*, 2006, **16**, 2871–2883.
3 H. Sohn, R. M. Calhoun, M. J. Sailor and W. C. Trogler, *Angew. Chem., Int. Ed.*, 2001, **40**, 2104–2105.
4 A. W. Czarnik, *Nature*, 1998, **394**, 417–418.
5 Y. Peng, A.-J. Zhang, M. Dong and Y.-W. Wang, *Chem. Commun.*, 2011, **47**, 4505–4507.
6 X.-G. Hou, Y. Wu, H.-T. Cao, H.-Z. Sun, H.-B. Li, G.-G. Shan and Z.-M. Su, *Chem. Commun.*, 2014, **50**, 6031–6034.
7 M. Nipper, Y. Qian, R. S. Carr and K. Miller, *Chemosphere*, 2004, **56**, 519–530.
8 S. Shanmugaraju, S. A. Joshi and P. S. Mukherjee, *J. Mater. Chem.*, 2011, **21**, 9130–9138.
9 J. Wyman, M. Serve, D. Hobson, L. Lee and J. Uddin, *J. Toxicol. Environ. Health, Part A*, 1992, **37**, 313.
10 D. T. McQuade, A. E. Pullen and T. M. Swager, *Chem. Rev.*, 2000, **100**, 2537–2574.
11 M. E. Germain and M. J. Knapp, *Chem. Soc. Rev.*, 2009, **38**, 2543–2555.
12 Y. H. Lee, H. Liu, J. Y. Lee, S. H. Kim, S. K. Kim, J. L. Sessler, Y. Kim and J. S. Kim, *Chem.–Eur. J.*, 2010, **16**, 5895–5901.
13 A. W. Martinez, S. T. Phillips, M. J. Butte and G. M. Whitesides, *Angew. Chem., Int. Ed.*, 2007, **46**, 1318–1320.
14 B. Roy, A. K. Bar, B. Gole and P. S. Mukherjee, *J. Org. Chem.*, 2013, **78**, 1306–1310.
15 A. Yadav and R. Boomishankar, *RSC Adv.*, 2015, **5**, 3903–3907.
16 R. Kumar, S. Sandhu, P. Singh, G. Hundal, M. S. Hundal and S. Kumar, *Asian J. Org. Chem.*, 2014, **3**, 805–813.
17 W. Wei, R. Lu, S. Tang and X. Liu, *J. Mater. Chem. A*, 2015, **3**, 4604–4611.
18 M. E. Walsh, *Talanta*, 2001, **54**, 427–438.
19 N. P. Saravanan, S. Venugopalan, N. Senthilkumar, P. Santhosh, B. Kavita and H. G. Prabu, *Talanta*, 2006, **69**, 656–662.

20 M. Krausa and K. Schorb, *J. Electroanal. Chem.*, 1999, **461**, 10–13.
21 S. Botti, L. Cantarini and A. Palucci, *J. Raman Spectrosc.*, 2010, **41**, 866–869.
22 X. Liu, L. Zhao, H. Shen, H. Xu and L. Lu, *Talanta*, 2011, **83**, 1023–1029.
23 H. H. Nguyen, X. Li, N. Wang, Z. Y. Wang, J. Ma, W. J. Bock and D. Ma, *Macromolecules*, 2009, **42**, 921–926.
24 R. Luggar, M. Farquharson, J. Horrocks and R. Lacey, *X Ray Spectrom.*, 1998, **27**, 87–94.
25 V. Anferov, G. Mozjoukhine and R. Fisher, *Rev. Sci. Instrum.*, 2000, **71**, 1656–1659.
26 W. J. Buttner, M. Findlay, W. Vickers, W. M. Davis, E. R. Cespedes, S. Cooper and J. W. Adams, *Anal. Chim. Acta*, 1997, **341**, 63–71.
27 K. Håkansson, R. V. Coorey, R. A. Zubarev, V. L. Talrose and P. Håkansson, *J. Mass Spectrom.*, 2000, **35**, 337–346.
28 J. L. Delaney, C. F. Hogan, J. Tian and W. Shen, *Anal. Chem.*, 2011, **83**, 1300–1306.
29 Z. Nie, F. Deiss, X. Liu, O. Akbulut and G. M. Whitesides, *Lab Chip*, 2010, **10**, 3163–3169.
30 R. B. Rucker, J. Zempleni, J. W. Suttie and D. B. McCormick, *Handbook of Vitamins*, CRC Press, 2007.
31 G. F. M. Ball, *Vitamins: Their Role in the Human Body*, Wiley-Blackwell, 2004.
32 G. F. Combs Jr and J. P. McClung, *The Vitamins: Fundamental Aspects In Nutrition And Health*, Academic Press, 2016.
33 *B. Pharmacopoeia*, Her Majesty's Stationary Office, London, UK, 2013.
34 G. Penzer and G. Radda, *Q. Rev., Chem. Soc.*, 1967, **21**, 43–65.
35 I. Ahmad, S. Ahmed, M. A. Sheraz, M. Aminuddin and F. H. M. Vaid, *Chem. Pharm. Bull.*, 2009, **57**, 1363–1370.
36 Y. Sato, M. Yokoo, S. Takahashi and T. Takahashi, *Chem. Pharm. Bull.*, 1982, **30**, 1803–1810.
37 M. A. Sheraz, S. H. Kazi, S. Ahmed, Z. Anwar and I. Ahmad, *Beilstein J. Org. Chem.*, 2014, **10**, 1999–2012.
38 E. Choe, R. Huang and D. B. Min, *J. Food Sci.*, 2005, **70**, R28–R36.
39 B. Gogoi and N. Sen Sarma, *ACS Appl. Mater. Interfaces*, 2015, **7**, 11195–11202.
40 B. Kalita, B. Gogoi and N. S. Sarma, *Mater. Res. Bull.*, 2019, **115**, 211–218.
41 R. Ouellette and J. D. Rawn, *Principles of Organic Chemistry*, 2015, vol. 1, pp. 287–314.
42 P. Dutta, D. Saikia, N. C. Adhikary and N. S. Sarma, *ACS Appl. Mater. Interfaces*, 2015, **7**, 24778–24790.
43 T. Chu, F. Zhang, Y. Wang, Y. Yang and S. W. Ng, *Chem.–Eur. J.*, 2017, **23**, 7748–7754.
44 J. R. Lakowicz, *Principles of Fluorescence Spectroscopy*, Springer Science & Business Media, 2013.
45 X. Sun, X. Ma, C. V. Kumar and Y. Lei, *Anal. Methods*, 2014, **6**, 8464–8468.
46 V. Kumar, A. Kumar, M. K. Chini and S. Satapathi, *Mater. Chem. Phys.*, 2021, **260**, 124130–124137.
47 B. Jiang, W. Liu, S. Liu and W. Liu, *Dyes Pigm.*, 2021, **184**, 108794–108798.
48 R. Singh, K. Mitra, S. Singh, S. Senapati, V. K. Patel, S. Vishwakarma, A. Kumari, J. Singh, S. K. S. Gupta and N. Misra, *Analyst*, 2019, **144**, 3620–3634.
49 R. Patel, S. Bothra, R. Kumar and S. K. Sahoo, *Nano-Struct. Nano-Objects*, 2019, **19**, 100345.
50 M. Shyamal, D. Das, P. Giri, S. Maity and A. Misra, *Mater. Today Chem.*, 2019, **14**, 100193.
51 P. Sakthivel, K. Sekar, S. Singaravadivel and G. Sivaraman, *ChemistrySelect*, 2019, **4**, 3817–3822.
52 V. Bharadwaj, J. E. Park, S. K. Sahoo and H. J. Choi, *ChemistrySelect*, 2019, **4**, 10895–10901.
53 H. M. Ahmed, M. Ghalia, W. Zahra and M. M. Ayad, *Spectrochim. Acta, Part A*, 2021, **260**, 119967–119969.